



LTB₄ and 5-oxo-EETE from extracellular vesicles stimulate neutrophils in granulomatosis with polyangiitis[§]

Marcin Surmiak,* Anna Gielicz,* Darko Stojkov,[†] Rafał Szatanek,[§]
Katarzyna Wawrzycka-Adamczyk,* Shida Yousefi,[†] Hans-Uwe Simon,[†] and Marek Sanak^{1,*}

Departments of Internal Medicine* and Clinical Immunology,[§] Jagiellonian University Medical College, Krakow, Poland; and Institute of Pharmacology,[†] University of Bern, Bern, Switzerland

ORCID IDs: 0000-0001-8396-1488 (M.S.); 0000-0002-2128-2145 (A.G.); 0000-0001-9243-3759 (D.S.); 0000-0003-1327-6092 (R.S.); 0000-0002-1439-1474 (K.W.A.); 0000-0002-9855-4305 (S.Y.); 0000-0002-9404-7736 (H.U.S.); 0000-0001-7635-8103 (M.S.)

Abstract Activation of neutrophils is an important mechanism in the pathology of granulomatosis with polyangiitis (GPA). In this study, we evaluated whether extracellular vesicles (EVs) circulating in the plasma of GPA patients could contribute to this process. EVs from the plasma of GPA patients in the active stage of the disease (n = 10) and healthy controls (n = 10) were isolated by ultracentrifugation and characterized by flow cytometry (CD63, CD8) and nanoparticle tracking analysis. Targeted oxylipin lipidomics of EVs was performed by HPLC-MS/MS. EV/oxylipin-induced neutrophil extracellular traps (NETs) were analyzed by confocal microscopy, and released double-stranded DNA (dsDNA) was quantified by PicoGreen fluorescent dye. Reactive oxygen species (ROS) production and neutrophils' EV binding/uptake were evaluated by flow cytometry. Brief priming with granulocyte-macrophage colony-stimulating factor was required for EV-mediated ROS production and dsDNA release. It was observed that priming also increased EV binding/uptake by neutrophils only for EVs from GPA patients. EVs from GPA patients had higher concentrations of leukotriene (LT)B₄ and 5-oxo-eicosatetraenoic acid (5-oxo-EETE) as compared with EVs from healthy controls. Moreover, neutrophils stimulated with LTB₄ or 5-oxo-EETE produced ROS and released dsDNA in a concentration-dependent manner. These results reveal the potential role of EVs containing oxylipin cargo on ROS production and NET formation by activated neutrophils.—Surmiak, M., A. Gielicz, D. Stojkov, R. Szatanek, K. Wawrzycka-Adamczyk, S. Yousefi, H-U. Simon, and M. Sanak. LTB₄ and 5-oxo-EETE from extracellular vesicles stimulate neutrophils in granulomatosis with polyangiitis. *J. Lipid Res.* 2020. 61: 1–9.

Supplementary key words neutrophil extracellular traps • reactive oxygen species • immunology • inflammation • eicosanoids • leukotrienes • leukotriene B₄ • 5-oxo-eicosatetraenoic acid

This work was supported by the National Centre of Science in Poland (Grant 2016/21/D/NZ6/02123 to M.S.) and Swiss National Science Foundation Grants 31003A_173215 (to S.Y.) and 310030_166473 (to H.U.S.). The authors declare that they have no conflicts of interest with the contents of the article.

Manuscript received 29 December 2018 and in revised form 8 November 2019.

Published, *JLR Papers in Press*, November 18, 2019

DOI <https://doi.org/10.1194/jlr.M092072>

Copyright © 2020 Surmiak et al. Published under exclusive license by The American Society for Biochemistry and Molecular Biology, Inc.

This article is available online at <http://www.jlr.org>

Granulomatosis with polyangiitis (GPA) is an infrequent autoimmune disease with still unknown etiology. Several hypotheses suggest that genetic factors like polymorphisms of the proteinase inhibitor α -1-antitrypsin, cytokine gene variants (IL-10), or some HLA genotypes might be associated with GPA (1, 2). According to the Chapel Hill Consensus Conference, among primary systemic vasculitides, GPA is an anti-neutrophil cytoplasmic antibody [with specificity for proteinase-3 (PR3)-ANCA or cANCA] associated vasculitis affecting small vessels. This definition implies the presence of circulating cANCA and the absence or paucity of immune complex deposits in areas of vasculitis by immunohistochemical studies of tissue specimens (3). Among the spectrum of cells participating in the pathophysiology of GPA, neutrophils play the most important role. The current paradigm of GPA assumes neutrophil activation by IgG anti-PR3 (cANCA), which requires direct recognition of PR3 via the Fab region of the antibody and interaction of the Fc part of the antibody with Fc γ Rs on the neutrophil surface (4, 5). This causes neutrophil activation, degranulation, generation of reactive oxygen species (ROS), and eventually transmigration through the endothelial cell layer (6–8). However, a novel mechanism of immune cell activation in the pathophysiology of autoimmune diseases like GPA can be linked to extracellular vesicles (EVs).

Abbreviations: BVAS, Birmingham Vasculitis Activity Score; cANCA, anti-neutrophil cytoplasmic antibody (cytoplasmic staining pattern); C5a, complement component 5a; dsDNA, double-stranded DNA; EV, extracellular vesicle; EV-GPA, extracellular vesicle isolated from the plasma of patients with granulomatosis with polyangiitis; EV-HC, extracellular vesicle isolated from the plasma of healthy controls; GM-CSF, granulocyte-macrophage colony-stimulating factor; GPA, granulomatosis with polyangiitis; LT, leukotriene; NET, neutrophil extracellular trap; NTA, nanoparticle tracking analysis; 5-oxo-EETE, 5-oxo-eicosatetraenoic acid; PPP, platelet-poor plasma; PR3, proteinase-3; ROS, reactive oxygen species.

¹To whom correspondence should be addressed.

e-mail: nfsanak@cyf-kr.edu.pl

[§] The online version of this article (available at <http://www.jlr.org>) contains a supplement.

EVs are a heterogeneous population of extracellular particles bound by a phospholipid bilayer. They are released by practically all types of cells and can be detected in various biological fluids. According to the current nomenclature, EVs are divided into main groups of exosomes and microparticles (9). Exosomes are small (50–150 nm) and are derived from the endocytic compartment. Microparticles are larger (100–1,000 nm) and produced by budding of the plasma membrane following a loss of asymmetric distribution of phospholipids and reorganization of the cytoskeleton (10). Because the distinction between these two populations of EVs is difficult, classification of EVs into exosomes or microparticles is rather dogmatic. Some studies show that proteins like CD63, CD81, or CD9 are mostly present in exosomes, likely reflecting their origin (11); whereas these markers can also be detected on larger EVs (12). It is now recognized that EVs are an integral part of the intercellular microenvironment and may act as regulators of cell-to-cell communication (10). EVs can deliver proteins to the target cells or may participate in transferring receptors between cells. Recently, we observed that tumor-derived EVs can induce monocyte/macrophage differentiation (13). It is interesting that EV content may differ from the parent cells; moreover, different stimuli may cause release of EVs with different cargo (14, 15). EVs can also contain DNA (including mitochondrial DNA), mRNA, and microRNA, but little is known as yet about EV lipidomics. Several studies on EV lipids showed that EVs can contain active enzymes linked to lipid metabolism, like 12-lipoxygenase, phospholipase A2, phospholipase C, and phospholipase D, or lipid mediators like leukotrienes (LTs) (16–20). The role of EVs in GPA and neutrophil activation, especially in the context of lipidomics is still unclear. In this study, we analyzed the potential of plasma-derived EVs of GPA patients to activate neutrophils by focusing on the oxylipin cargo of EVs. We observed that vesicles isolated from GPA patients and not from the healthy controls were able to activate neutrophils and form neutrophil extracellular traps (NETs). These data provide insights into the mechanism by which EVs could activate neutrophils and modulate innate immune response under pathological conditions.

MATERIALS AND METHODS

Patient recruitment and sample collection

We enrolled 10 treatment-naïve patients in the active stage of GPA and 10 healthy sex- and age-matched controls. Disease activity was evaluated using the Birmingham Vasculitis Activity Score (BVAS) version 3 (BVAS >1). Blood samples were collected in the morning, at least 12 h after a meal. Basic laboratory tests (complete blood count, C-reactive protein, anti-PR3 IgG level) were performed on all participants of the study at the time of collection of the peripheral blood. Written informed consent was obtained from all participants of the study and the study protocol was accepted by Jagiellonian University Ethic Committee abiding by the Declaration of Helsinki principles.

Neutrophil isolation

Neutrophils were isolated from healthy donors' peripheral blood and collected into Vacutainer tubes (BD Life Sciences, Franklin Lakes, NJ) using Histopaque-1077 gradient centrifugation (Sigma-Aldrich, St. Louis, MO) followed by lysis of the remaining erythrocytes with ammonium chloride buffer. Purity (>98%) of the neutrophil fraction was ascertained by flow cytometry and cell viability (>95%) was verified by trypan blue exclusion staining. Immediately after isolation, granulocytes were resuspended in X-VIVO 15 medium (Lonza, Basel, Switzerland).

EV isolation

EVs were isolated from the platelet-poor plasma (PPP) of 10 treatment-naïve patients with active GPA (BVAS 7–22) and 10 healthy sex- and age-matched controls by centrifugation. Blood samples were taken into Vacutainer tubes with sodium citrate as anticoagulant. After blood collection, samples were centrifuged for 10 min at 1,450 *g* (continuously) to obtain plasma; the upper three-fourths of the plasma was collected and centrifuged again to obtain PPP (5,000 *g* for 5 min continuously). PPP was aliquoted and stored at –80°C. Frozen PPP (2.5 ml) was thawed in a water bath for 10 min at 25°C and centrifuged for 20 min at 3,500 *g* to remove any cryoprecipitate. For EV isolation, collected supernatant was diluted with PBS (7 ml total sample volume) and passed through 0.8 µm syringe filter. Purification of EVs was done by ultracentrifugation in a SORVALL WX 80+ ultracentrifuge and T-1270 fixed angle rotor (Thermo Fisher Scientific, Waltham, MA). EVs were pelleted by ultracentrifugation (1.5 h, 100,000 *g*), washed with PBS, and centrifuged again (1.5 h, 100,000 *g*). The EV pellet was next suspended in 250 µl of filtered PBS, aliquoted, and stored at –80°C for experiments.

EV size distribution and surface marker characterization

EV number and size distribution was measured using nanoparticle tracking analysis (NTA) (NanoSight LM10; Malvern Instruments, Amesbury, UK). EV samples were diluted 1:1,000 with filtered PBS to reduce their number to the linear range of the apparatus, i.e., below $2-10 \times 10^8$ /ml. Measurement video images were analyzed using NTA 3.1 Build 3.1.46 software (Malvern) captured in script control mode (three videos of 60 s per measurement) using the syringe pump speed 80. A total of 1,500 frames were examined per sample.

To rule out any presence of stimulatory endotoxins or anti-PR3 IgG (cANCA) antibodies derived from the plasma of GPA patients, EV specimens were tested by a colorimetric method detecting bacterial endotoxins (Pierce Chromogenic Endotoxin Quant kit; Thermo Fisher Scientific, Waltham, MA) and by an indirect immunofluorescence method detecting cANCA (ANCA IFA Granulocyte BIOCHIP Mosaic test; EUROIMMUN, Germany).

Evaluation of EV surface markers was performed by flow cytometry as previously described (21, 22). Briefly, EV aliquots (10 µl) were resuspended in PBS, mixed with 5 µl of aldehyde/sulfate-latex beads (4 µm in diameter; Invitrogen, Carlsbad, CA) and incubated at room temperature for 15 min in a 1.5 ml Eppendorf tube. After incubation, the content was added with 1 ml of 2% BSA in PBS and incubated overnight with rotation at 4°C. Bead-coupled EVs were pelleted by centrifugation at 2,700 *g* for 5 min, washed with 1 ml of 2% BSA in PBS, and centrifuged again. The pellet was resuspended with 50 µl of PBS and stained with the antibodies, anti-CD63 (FITC, BD Biosciences) and anti-CD81 (PerCP-eFluor 710; Thermo Fisher Scientific), for 30 min at room temperature.

Gating of EV-decorated latex beads was on forward/side scatter parameters, thus unbound EVs or antibody aggregates were excluded from the analysis (supplemental Fig. S1).

Targeted oxylipin lipidomics of EVs was performed by HPLC-MS/MS. Briefly, samples were enriched with chemically identical deuterated standards (Cayman Chemical Co., Ann Arbor, MI), extracted to an organic phase, and analyzed using multiple reaction monitoring mode MS/MS (Qtrap 4000; Applied Biosystems). Details on the analytical procedure are provided in the supplemental information, supplemental Tables S1 and S2, and supplemental Figs. S2–S4.

ROS production

Generation of ROS was measured in granulocytes by flow cytometry using dihydrorhodamine 123. Isolated granulocytes ($2 \times 10^5/225 \mu\text{l}$ in X-VIVO 15 medium) were stained with dihydrorhodamine 123 ($5 \mu\text{g/ml}$; Sigma-Aldrich) during a 5 min incubation at 37°C with gentle shaking (150 rpm). Next, neutrophils were primed with recombinant granulocyte-macrophage colony-stimulating factor (GM-CSF) (25 ng/ml ; R&D Systems, Minneapolis, MN) or left without priming for 15 min at 37°C and then stimulated with the complement component 5a (C5a) fragment (positive control, 10^{-8} M), EVs from GPA patients or healthy controls ($25 \mu\text{l}$), 5-oxo-eicosatetraenoic acid (5-oxo-EETE), or LTB_4 ($4\text{--}400 \text{ pg/ml}$; Cayman Chemical Co.). After 1 h, stimulation was stopped by addition of ice-cold PBS. ROS activity of the samples was measured immediately by flow cytometry (BD FACSCanto II) as rhodamine mean fluorescence intensity.

EV binding/uptake by neutrophils

EV specimens were stained with PKH67 fluorescent tracker dye (PKH67 Fluorescent Cell Linker Kit; Sigma-Aldrich) for 5 min in 37°C . The staining reaction was stopped by addition of PBS with 1% BSA and removal of unbound dye by three cycles of washing/centrifugation using Amicon Ultra 0.5 ml centrifugal filters (100K; Merck-Millipore, Billerica, MA). After the final centrifugation, EV concentrates were restituted to their original volume.

The presence of PKH67-labeled EVs in granulocytes was measured by flow cytometry (BD FACSCanto II). Neutrophils isolated from healthy donors ($0.2 \times 10^6/225 \mu\text{l}$) were primed with GM-CSF (25 ng/ml) or left without priming for 15 min at 37°C and then incubated with EVs ($25 \mu\text{l}$) for 1 h. After stimulation, cells were washed twice by centrifugation, resuspended in PBS, and analyzed.

Quantification of dsDNA release by stimulated human neutrophils

Isolated human neutrophils ($5 \times 10^5/225 \mu\text{l}$ in X-VIVO 15 medium) were primed with recombinant GM-CSF (25 ng/ml ; R&D Systems) or left unprimed for 15 min at 37°C and then stimulated with the C5a fragment (positive control, 10^{-8} M). EVs from GPA patients or healthy controls ($25 \mu\text{l}$), 5-oxo-EETE, or LTB_4 ($4\text{--}400 \text{ pg/ml}$; Cayman Chemical Co.) to activate the cells for 1 h. After the incubation, DNase I (EURx, Gdansk, Poland) was added at 2.5 U/ml concentration for the next 10 min. The reaction was stopped by addition of 2.5 mM EDTA, pH 8.0 (Sigma-Aldrich). Cells were centrifuged at $190 g$ for 5 min at 4°C . The content of double-stranded DNA (dsDNA) in the supernatant was measured using Quant-iT Pico Green dsDNA assay kit and a Qubit 3 fluorimeter (Thermo Fisher Scientific).

Visualization of NET formation

Isolated granulocytes were resuspended in X-VIVO 15 medium ($2.5 \times 10^6/\text{ml}$). Cells were primed with 25 ng/ml GM-CSF for 20 min on cleaned glass coverslips. Glass pretreatment included washes with acetone, ethanol, deionized water, and baking at 200°C for 1 h. Cells were incubated with 10^{-8} M C5a or EVs ($25 \mu\text{l}$) from GPA patients or healthy controls for 1 h at 37°C in

$5\% \text{ CO}_2$. After stimulation, staining of live cells with a cell-permeable fluorescent dye, MitoSOX Red ($5 \mu\text{M}$), was performed. Cells were next fixed with 4% paraformaldehyde for 5 min, washed three times in PBS, and counterstained with $1 \mu\text{g/ml}$ Hoechst 33342, and then mounted in ProLong Gold medium. Slides were examined and images acquired by confocal laser scanning microscopy (LSM 700; Carl Zeiss Micro Imaging, Jena, Germany) or DMi8 S Platform (Leica Microsystems, Wetzlar, Germany).

Statistical analysis

Statistical analysis was performed using GraphPad Prism 5.0 software (GraphPad Software Inc, San Diego, CA). All comparisons were done using one-way ANOVA with Tukey's post hoc test or Student's *t*-test and Mann-Whitney U test. Descriptive statistics were presented as a mean \pm SD or median \pm interquartile range. Type I statistical error $P < 0.05$ was considered significant.

RESULTS

The study subjects and EV characteristics

All GPA patients were newly diagnosed and treatment naïve, and were anti-PR3 IgG positive. The BVAS disease activity score was between 7 and 22 (median = 14). Clinical laboratory tests showed that in comparison with healthy controls, GPA patients had an elevated number of polymorphonuclear leukocytes and peripheral blood mononuclear cells (supplemental Table S3).

EVs isolated from GPA patients (EV-GPAs) or healthy controls (EV-HCs) were in the same size range and concentration (Fig. 1A, B). Moreover, there were no differences in expression of EV markers. Both EV-GPAs and EV-HCs expressed CD63 and CD81 (Fig. 1C). All EV samples were free of IgG anti-PR3 antibodies and bacterial endotoxins.

EV-mediated neutrophil activation

To evaluate whether plasma-derived EVs can participate in the granulocyte activation observed in GPA, we performed experiments in which neutrophils isolated from healthy donors were stimulated with EVs. Using our preparatory technique, EVs were $10\times$ concentrated because $250 \mu\text{l}$ of EVs in PBS were obtained from 2.5 ml of PPP. To mimic EV abundance in plasma, neutrophils were stimulated with $25 \mu\text{l}$ of EVs diluted 10-fold in the total cell suspension volume. First, neutrophils were stimulated with EV-GPAs or EV-HCs alone. No differences were noticed between cells stimulated with EV-GPAs or EV-HCs and cell culture medium used as negative control. For the next experiments, neutrophils were primed with GM-CSFs (25 ng/ml) before addition of EVs. Following stimulation with EVs, ROS production (Fig. 2A) and release of dsDNA (Fig. 2B) were observed. These results were present only when EV-GPAs were used. Stimulation of primed neutrophils by EV-HCs resulted in the absence of ROS production or dsDNA release. Moreover, direct microscopy showed that DNA released by intact live neutrophils stimulated with EV-GPAs was likely of mitochondrial origin (Fig. 2C). To analyze how priming can influence EV-mediated activation of neutrophils, we compared primed or unprimed cells incubated with EVs stained by fluorescent tracker (PKH67).

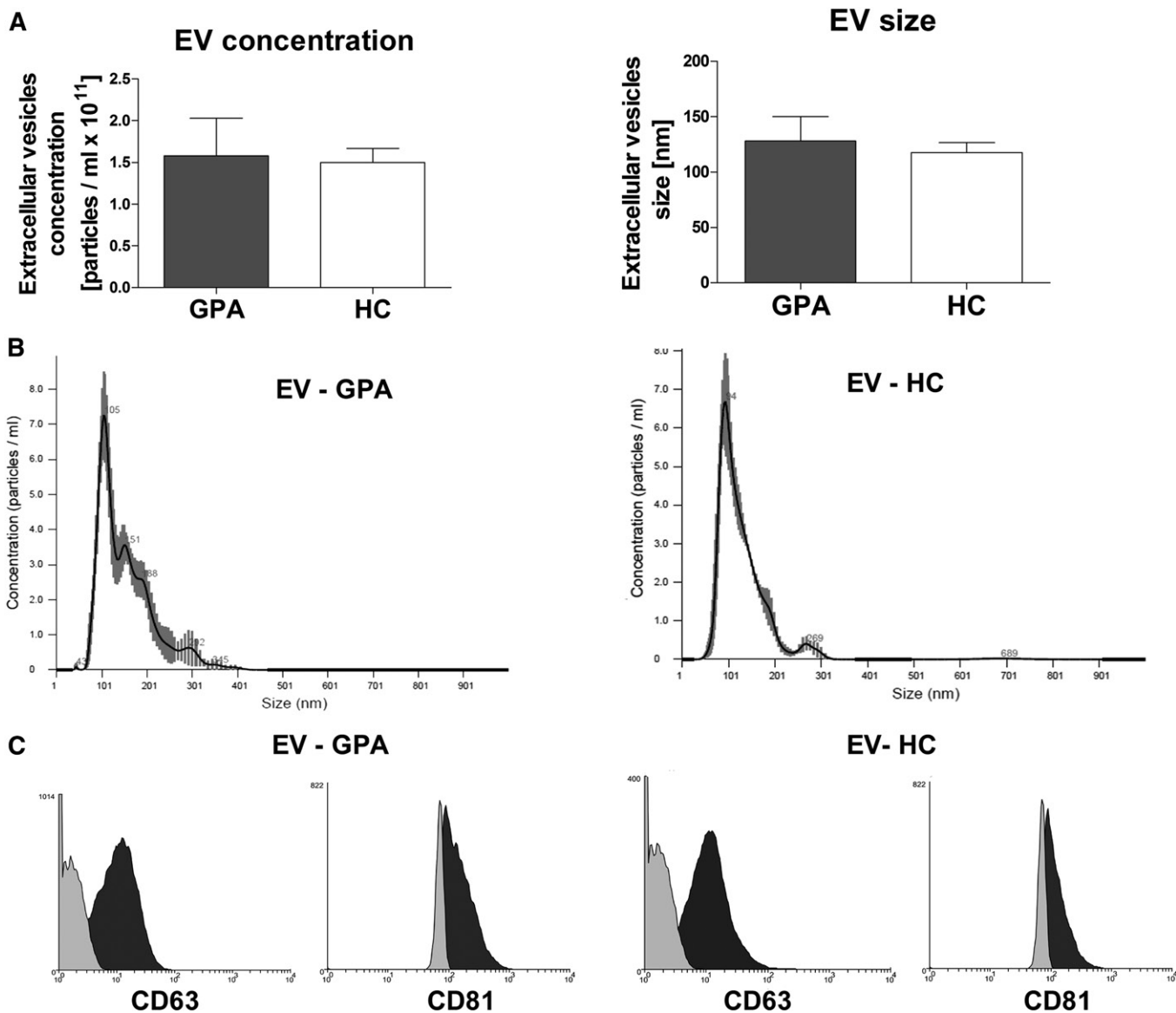


Fig. 1. A: Concentration and size distribution of plasma-derived EVs. Results are presented as mean \pm SD. B, C: Representative histograms of size distribution (B) and CD63/CD81 expression (C) of EVs. Left panels: EVs isolated from GPA patient. Right panels: EVs isolated from healthy donor. In panel C, light gray indicates isotype control; dark gray indicates CD63 or CD81.

Binding or uptake of EVs was evaluated by flow cytometry. We observed that the percentage of PKH67-positive cells (neutrophils/EV aggregates) was higher for primed cells; however, this was evident only for EV-GPAs (PKH67-positive cells: primed vs. unprimed, $P < 0.05$; **Fig. 3**, supplemental Fig. S5).

Targeted oxylipin lipidomics of EVs

To identify putative stimuli causing neutrophil activation, we performed targeted oxylipin analysis of EVs using HPLC-MS/MS. Out of 14 quantified oxylipins, the lowest concentration in EVs was observed for LTC₄ (EV-GPAs 16.2 ± 8.5 pg/ml vs. EV-HCs 16.0 ± 8.2 pg/ml; $P > 0.05$; supplemental Fig. S6) and the highest for 13,14-dihydro-15-keto PGE₂ (EV-GPAs 818 ± 448 pg/ml vs. EV-HCs 819 ± 448 pg/ml, $P > 0.05$, supplemental Fig. S6). Significant differences between EV-GPAs and EV-HCs were present for LTB₄ (EV-GPAs: 470 ± 176 vs. EV-HCs: 215 ± 107 pg/ml;

$P < 0.05$), 5-oxo-EETE (EV-GPAs 524 ± 279 pg/ml vs. EV-HCs 221 ± 81.2 pg/ml; $P < 0.05$), and 5-HETE (EV-GPAs 62.9 ± 31 pg/ml vs. EV-HCs 28.9 ± 15.7 pg/ml; $P < 0.05$) (**Fig. 4**).

Oxylipin-mediated neutrophil activation

To confirm the functional importance of the more abundant oxylipins in EV-GPAs, we stimulated neutrophils for ROS production and dsDNA release with pure chemical LTB₄ and 5-oxo-EETE. 5-HETE, the precursor of 5-oxo-EETE, had no activity at the measured concentration (supplemental Fig. S7). Stimulation of neutrophils with escalated concentrations of LTB₄ or 5-oxo-EETE increased ROS production or release of dsDNA at the minimal concentration of 4 pg/ml. The peak levels of ROS were observed in cells stimulated with 40 pg/ml of LTB₄ or 5-oxo-EETE (**Fig. 5A**). The highest levels of dsDNA release occurred after stimulation of granulocytes with 400 pg/ml of LTB₄ or 5-oxo-EETE

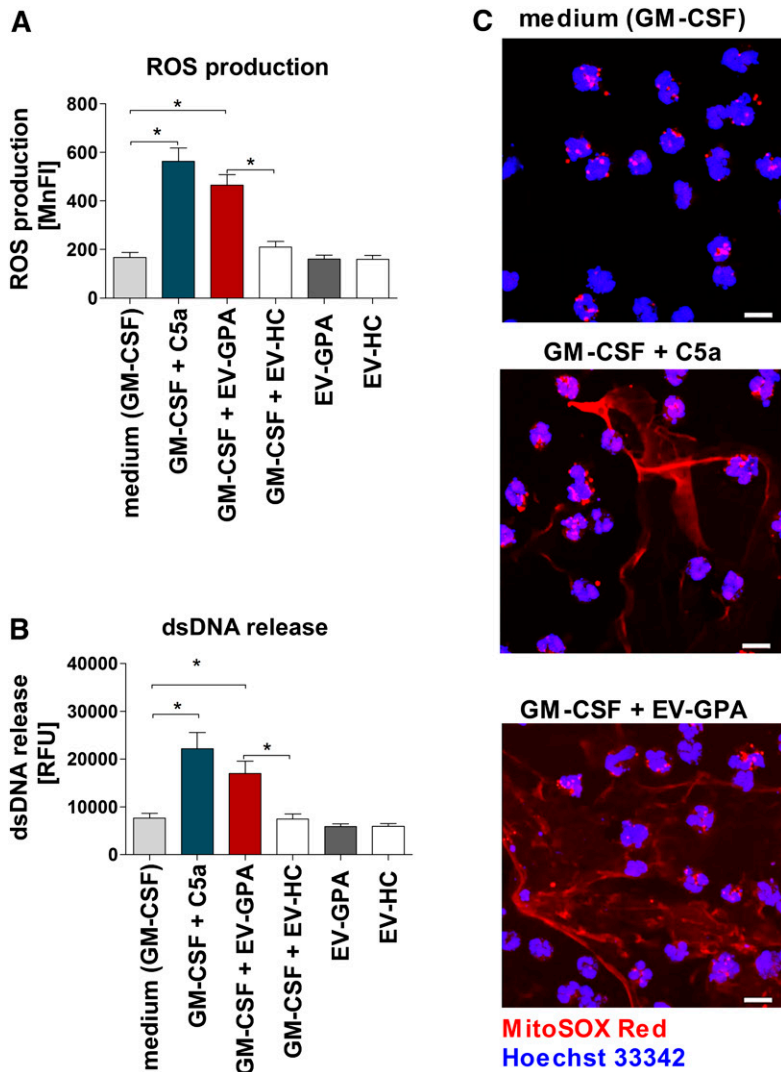


Fig. 2. EVs isolated from GPA patients activate human neutrophils. Neutrophils were isolated from the blood of healthy donors ($n = 6$) and stimulated with C5a (positive control) or EV-GPAs ($n = 10$) and healthy controls (EV-HC; $n = 10$). In each experiment, cells were primed (GM-CSF, 25 ng/ml) or left unprimed for 15 min before stimulation in parallel experiments with EV-GPAs or EV-HCs. Each EV sample was tested with neutrophils from two different donors. **A:** Total ROS production by activated neutrophils was measured by flow cytometry. **B:** Quantification of dsDNA in supernatants of activated neutrophils was performed using PicoGreen fluorescent dye. **C:** Confocal microscopy. Representative images of extracellular DNA release following short-term stimulation (total 45 min) of human neutrophils with the stimuli. Cells were labeled with 5 μ M of MitoSOX Red to stain the extracellular DNA and the cell nucleus was stained with 1 μ g/ml Hoechst 33342. Scale bars are 10 μ m. The images were acquired by confocal scanning microscope. Results are presented as mean \pm SD of mean fluorescence intensity (MnFI) or relative fluorescence units (RFU) and were tested with the use of ANOVA with Tukey's post hoc test. * $P < 0.05$ compared with nonstimulated control.

(Fig. 5B). However, like EV-GPA stimulation, neutrophil activation by LTB₄ or 5-oxo-EETE required prior GM-CSF priming (Fig. 5C).

DISCUSSION

Circulating EVs have already been suggested to participate in the pathophysiology of autoimmune diseases, including GPA. However, most of the previous studies were limited to the descriptive observations. Hong et al. (23) showed that neutrophils stimulated with ANCA antibodies can release microparticles activating endothelial cells. Daniel et al. (24) reported higher plasma levels of circulating EVs in patients with an active stage of GPA. In contrast to the latter observation, we failed to observe any differences between the concentration of EVs isolated from the plasma of GPA patients or healthy controls. This discrepancy could result from a different methodological approach. Daniel et al. (24) used low-speed (15,000 g) centrifugation as the isolation method and direct analysis with the use of flow cytometry but no NTA or transmission electron microscopy analysis. Possibly, researchers focused on populations of

large EVs, like microparticles and apoptotic bodies. In the current study, ultracentrifugation was used for isolation and NTA analysis confirmed the enrichment of small EVs; this could explain the difference between the counting of large EVs in the previous study and a population of small exosomes and microparticles in the current one.

Studies on EVs are currently a very popular research area because the contribution of EVs in the pathophysiology of several disorders has been confirmed (25–28). However, interactions of EVs with granulocytes, especially in autoimmune diseases like GPA, are poorly investigated. The study of Kuravi et al. (16) showed that platelet-derived EVs can promote adhesion of neutrophils to endothelial cells. Dieker et al. (29) reported that circulating microparticles isolated from patients with systemic lupus erythematosus participate in NET formation by LPS-stimulated cells. Release of dsDNA by activated neutrophils was also observed in cells stimulated with small EVs (30–150 nm) isolated from the cell culture supernatants of cancer cells (30). Interestingly, formation of NETs by activated neutrophils originally was considered to be one of the neutrophil death pathways, involving the rearrangement of nuclear and granular architecture that proceeded from the dissolution

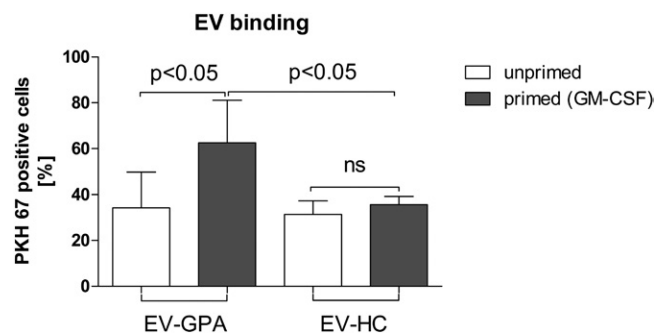


Fig. 3. Binding of EVs to primed and unprimed neutrophils. Neutrophils isolated from the blood of healthy donors ($n = 6$) were primed with GM-CSF or left unprimed for 15 min at 37°C . Neutrophils were next added with PKH67-stained EVs (isolated from GPA patients or healthy controls) for 1 h. Results are presented as median \pm interquartile range of PKH67-positive cells and were tested with the use of ANOVA with Tukey's post hoc test. A control of unprimed neutrophils was added with non-stained EVs (for gating strategy see supplemental Fig. S5).

of internal membranes to chromatin decondensation, cytolysis, and the formation of nuclear DNA fibers traps (31–33). However, we reported that neutrophils can form NETs consisting of mitochondrial DNA in a ROS-dependent mechanism and remain viable (34, 35). This observation may shed light on the persistence of innate immune response activation in autoimmune disorders.

The mechanism of activation of neutrophils in GPA involves the binding of self-reactive anti-PR-3 antibodies, which stimulate these cells (4, 5, 36). In the present study, stimulation with small EVs isolated from the plasma of GPA patients led to ROS production and release of dsDNA in GM-CSF-primed neutrophils. The requirement for the neutrophil priming was met by preincubation with GM-CSF prior to stimulation. Higher levels of priming cytokines like TNF- α and GM-CSF were previously documented in

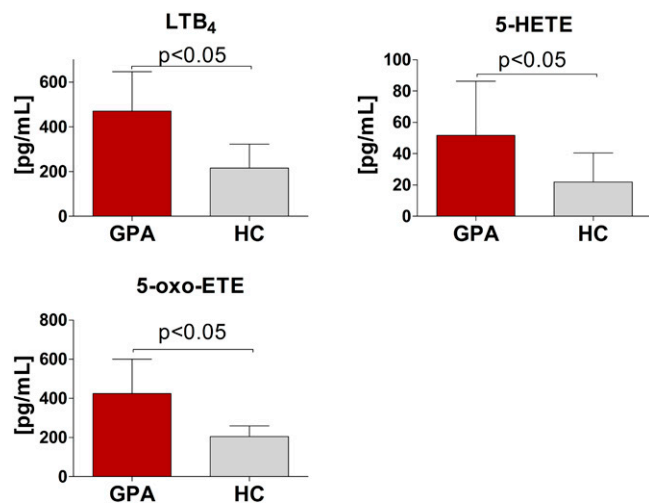


Fig. 4. EV levels of LTB₄, 5-HETE, and 5-oxo-EETE. EVs were isolated from the plasma of patients with GPA ($n = 10$) and healthy controls (HC; $n = 10$) and targeted oxylipin lipidomics of EVs was performed by HPLC-MS/MS. Results are presented as mean \pm SD. Differences between the studied groups were tested with the use of Student's *t*-test.

GPA by us and others, and these observations may explain the occurrence of priming effects in vivo (37, 38). Moreover, we reported that the level of circulating cell-free mitochondrial DNA is higher in comparison with healthy controls in patients with GPA (39). Taken together, the presented results demonstrate that NETs could be an important mechanism of granulocyte activation in the pathophysiology of GPA. Because neutrophils are key players in the pathophysiology of GPA, the current findings expand the knowledge supporting this idea.

In addition to the increased binding and uptake of EVs by primed granulocytes, the cells' activation may result from the oxylipins' cargo of EVs. This has been shown before in studies on LTB₄ or 5-oxo-EETE-mediated neutrophil aggregation, adherence, calcium mobilization, ROS production, or chemotaxis. All of these effects required priming of neutrophils with GM-CSF or TNF- α (40–44). Our results on LTB₄ and 5-oxo-EETE stimulation are in line with these studies. The novel finding of the current study is that EV stimulation caused release of dsDNA along with ROS production. This was detectable when primed granulocytes were stimulated with LTB₄ or 5-oxo-EETE; moreover, only EV-GPA had these stimulatory properties, containing a doubled cargo of LTB₄ and 5-oxo-EETE. We also noticed that EV-HCs, in which the concentration of LTB₄ and 5-oxo-EETE was theoretically sufficient for granulocyte activation, did not stimulate primed cells to ROS production or dsDNA release. This could be explained by several factors. First, due to the complexity of the EV cargo, EV-HCs can contain molecules suppressing neutrophil activation. The anti-inflammatory potential of EVs has been reported for neutrophil-derived microparticles isolated from healthy donors or rheumatoid arthritis patients (45, 46). Second, EV-HCs might be deficient in some target molecules crucial for internalization by granulocytes. Duchez et al. (47) reported that active 12-lipoxygenase was essential for the internalization of platelet-derived EVs by neutrophils, while the studies of Maugeri and colleagues showed that this process required the presence of high mobility group box 1 (HMGB1), which was absent in microparticles isolated from healthy donors (48, 49). In the current study, we did not analyze any potential proteins involved in EV uptake by granulocytes. However, we observed that priming of neutrophils with GM-CSF resulted in increased EV binding/uptake only for EV-GPAs, explaining the lack of EV-mediated neutrophil activation when EV-HCs were used. However, only experiments using antagonists of the receptors BLT1, BLT2, and OXER1 could provide additional evidence to confirm the specific role of these two oxylipins.

The mechanism of release and intracellular origin of small EVs is difficult to study *ex vivo*; thus, a cellular source of plasma circulating EVs remains uncertain. In contrast to large microparticles, classical lineage membrane markers like CD11b for granulocytes or CD42a for platelets cannot be used (50). However, some previous studies provided information on the origin of EVs by their oxylipin content (51, 52). Duchez et al. (47) reported that in platelet-derived exosomes, the main arachidonic acid metabolite is 12-HETE. In our study, high levels of LTB₄ and 5-oxo-EETE

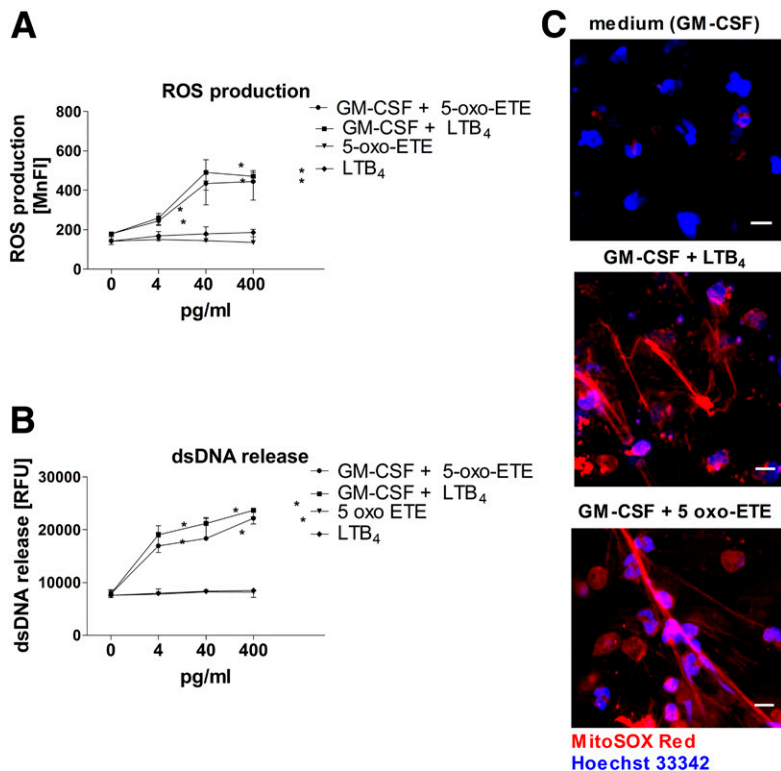


Fig. 5. ROS production (A) and dsDNA release (B, C) by human neutrophils primed with GM-CSF and stimulated with LTB₄ or 5-oxo-EETE. A, B: Neutrophils isolated from the blood of healthy donors ($n = 6$) were primed with GM-CSF (25 ng/ml) or left unprimed for 15 min at 37°C, and then stimulated with serial dilutions of 5-oxo-EETE or LTB₄. The concentration of 40 pg/ml for 5-oxo-EETE or LTB₄ is representative of the mean concentration of both eicosanoids in experiments in which cells were stimulated with plasmas-derived EVs isolated from patients with GPA. C: Fluorescence microscopy. Representative images of extracellular DNA release following short-term stimulation (total 45 min) of human neutrophils with the indicated stimuli. Cells were labeled with 5 μ M of MitoSOX Red to stain the extracellular DNA, and the nucleus was stained with 1 μ g/ml Hoechst 33342. Scale bars are 10 μ m. The images were acquired by fluorescence microscope (DMi8; Leica). The results are presented as mean \pm SD and were tested with the use of ANOVA and Tukey's post hoc test. * $P < 0.05$ compared with nonstimulated control.

were detected, produced by 5-lipoxygenase-positive (ALOX-5) granulocytes. The 5-lipoxygenase is also expressed in monocytes, macrophages, and dendritic cells (53–55). The study by Esser et al. (17) suggested LTC₄ as the main eicosanoid in exosomes from macrophages and dendritic cells; whereas more recently, Majumdar, Tavakoli Tameh, and Parent (56) reported that during chemotaxis neutrophils release LTB₄-enriched EVs. Interestingly enough, 5-oxo-EETE is the major metabolite of 5-HETE formed during ROS production in neutrophils (57). We previously published an article on the increased biosynthesis of these two mediators in asthmatics following a positive challenge with a house dust mite allergen, which correlated with the late phase of allergic inflammation (58). Taken together, it is highly plausible that granulocytes are the main source of small EVs in patients with GPA. We acknowledge that this study lacked appropriate methods to evaluate the mechanism of EV formation ex vivo, and this will require future investigations.

In conclusion, we described a novel observation that primed neutrophils can be stimulated by circulating EV-GPAs to produce ROS and release dsDNA. Moreover, by targeted lipidomics, we demonstrated that pro-inflammatory oxylipins of the 5-lipoxygenase pathway had increased concentration in EV-GPAs, and their activity could be mimicked by chemically pure LTB₄ or 5-oxo-EETE. The current results also confirm that release of dsDNA by NET formation is an important mechanism of neutrophil activation in the pathophysiology of GPA. [Fig 5](#)

Images were acquired on equipment supported by the Microscopy Imaging Centre of the University of Bern.

REFERENCES

- Gencik, M., S. Borgmann, R. Zahn, E. Albert, T. Sitter, J. T. Epplen, and H. Fricke. 1999. Immunogenetic risk factors for anti-neutrophil cytoplasmic antibody (ANCA)-associated systemic vasculitis. *Clin. Exp. Immunol.* **117**: 412–417.
- Muraközy, G., K. I. Gaede, B. Ruprecht, O. Gutzeit, M. Schürmann, A. Schnabel, M. Schlaak, W. L. Gross, and J. Müller-Quernheim. 2001. Gene polymorphisms of immunoregulatory cytokines and angiotensin-converting enzyme in Wegener's granulomatosis. *J. Mol. Med. (Berl.)* **79**: 665–670.
- Kettritz, R., J. C. Jennette, and R. J. Falk. 1997. Crosslinking of ANCA-antigens release by human neutrophils stimulates superoxide. *J. Am. Soc. Nephrol.* **8**: 386–394.
- Surmiak, M., M. Kaczor, and M. Sanak. 2015. Proinflammatory genes expression in granulocytes activated by native proteinase-binding fragments of anti-proteinase 3 IgG. *J. Physiol. Pharmacol.* **66**: 609–615.
- Surmiak, M., M. Kaczor, and M. Sanak. 2012. Expression profile of proinflammatory genes in neutrophil-enriched granulocytes stimulated with native anti-PR3 autoantibodies. *J. Physiol. Pharmacol.* **63**: 249–256.
- Mulder, A. H., P. Heeringa, E. Brouwer, P. C. Limburg, and C. G. Kallenberg. 1994. Activation of granulocytes by anti-neutrophil cytoplasmic antibodies (ANCA): a Fc gamma RII-dependent process. *Clin. Exp. Immunol.* **98**: 270–278.
- Chen, M., and C. G. Kallenberg. 2010. ANCA-associated vasculitides—advances in pathogenesis and treatment. *Nat. Rev. Rheumatol.* **6**: 653–664.
- Rarok, A. A., P. C. Limburg, and C. G. M. Kallenberg. 2003. Neutrophil-activating potential of antineutrophil cytoplasm autoantibodies. *J. Leukoc. Biol.* **74**: 3–15.
- van der Pol, E., A. N. Böing, P. Harrison, A. Sturk, and R. Nieuwland. 2012. Classification, functions, and clinical relevance of extracellular vesicles. *Pharmacol. Rev.* **64**: 676–705.
- Colombo, M., G. Raposo, and C. Théry. 2014. Biogenesis, secretion, and intercellular interactions of exosomes and other extracellular vesicles. *Annu. Rev. Cell Dev. Biol.* **30**: 255–289.
- Akers, J. C., D. Gonda, R. Kim, B. S. Carter, and C. C. Chen. 2013. Biogenesis of extracellular vesicles (EV): exosomes, microvesicles, retrovirus-like vesicles, and apoptotic bodies. *J. Neurooncol.* **113**: 1–11.

12. Crescitelli, R., C. Lässer, T. G. Szabó, A. Kittel, M. Eldh, I. Dianzani, E. I. Buzás, and J. Lötvall. 2013. Distinct RNA profiles in subpopulations of extracellular vesicles: apoptotic bodies, microvesicles and exosomes. *J. Extracell. Vesicles*. **2**.
13. Baj-Krzyworzeka, M., B. Mytar, R. Szatanek, M. Surmiak, K. Węglarczyk, J. Baran, and M. Siedlar. 2016. Colorectal cancer-derived microvesicles modulate differentiation of human monocytes to macrophages. *J. Transl. Med.* **14**: 36.
14. Valadi, H., K. Ekström, A. Bossios, M. Sjöstrand, J. J. Lee, and J. O. Lötvall. 2007. Exosome-mediated transfer of mRNAs and microRNAs is a novel mechanism of genetic exchange between cells. *Nat. Cell Biol.* **9**: 654–659.
15. Dalli, J., T. Montero-Melendez, L. V. Norling, X. Yin, C. Hinds, D. Haskard, M. Mayr, and M. Perretti. 2013. Heterogeneity in neutrophil microparticles reveals distinct proteome and functional properties. *Mol. Cell. Proteomics*. **12**: 2205–2219.
16. Kuravi, S. J., P. Harrison, G. E. Rainger, and G. B. Nash. 2019. Ability of platelet-derived extracellular vesicles to promote neutrophil-endothelial cell interactions. *Inflammation*. **42**: 290–305.
17. Esser, J., U. Gehrmann, F. L. D’Alexandri, A. M. Hidalgo-Estévez, C. E. Wheelock, A. Scheynius, S. Gabriellsson, and O. Rådmark. 2010. Exosomes from human macrophages and dendritic cells contain enzymes for leukotriene biosynthesis and promote granulocyte migration. *J. Allergy Clin. Immunol.* **126**: 1032–1040.
18. Record, M., K. Carayon, M. Poirot, and S. Silvente-Poirot. 2014. Exosomes as new vesicular lipid transporters involved in cell–cell communication and various pathophysiological. *Biochim. Biophys. Acta*. **1841**: 108–120.
19. Skotland, T., K. Sandvig, and A. Llorente. 2017. Lipids in exosomes: current knowledge and the way forward. *Prog. Lipid Res.* **66**: 30–41.
20. Subra, C., D. Grand, K. Laulagnier, A. Stella, G. Lambeau, M. Paillasse, P. De Medina, B. Monsarrat, B. Perret, S. Silvente-Poirot, et al. 2010. Exosomes account for vesicle-mediated transcellular transport of activatable phospholipases and prostaglandins. *J. Lipid Res.* **51**: 2105–2120.
21. Osteikoetxea, X., A. Balogh, K. Szabó-Taylor, A. Németh, T. G. Szabó, K. Pálóczi, B. Sódar, Á. Kittel, B. György, É. Pállinger, et al. 2015. Improved characterization of EV preparations based on protein to lipid ratio and lipid properties. *PLoS One*. **10**: e0121184.
22. Suárez, H., A. Gámez-Valero, R. Reyes, S. López-Martín, M. J. Rodríguez, J. L. Carrascosa, C. Cabañas, F. E. Borràs, and M. Yáñez-Mó. 2017. A bead-assisted flow cytometry method for the semi-quantitative analysis of extracellular vesicles. *Sci. Rep.* **7**: 11271.
23. Hong, Y., D. Eleftheriou, A. A. Hussain, F. E. Price-Kuehne, C. O. Savage, D. Jayne, M. A. Little, A. D. Salama, N. J. Klein, and P. A. Brogan. 2012. Anti-neutrophil cytoplasmic antibodies stimulate release of neutrophil microparticles. *J. Am. Soc. Nephrol.* **23**: 49–62.
24. Daniel, L., F. Fakhouri, D. Joly, L. Mouthon, P. Nusbaum, J-P. Grunfeld, J. Schifferli, L. Guillemin, P. Lesavre, and L. Halbwachs-Mecarelli. 2006. Increase of circulating neutrophil and platelet microparticles during acute vasculitis and hemodialysis. *Kidney Int.* **69**: 1416–1423.
25. Eguchi, A., and A. E. Feldstein. 2018. Extracellular vesicles in non-alcoholic and alcoholic fatty liver diseases. *Liver Res.* **2**: 30–34.
26. Letsiou, E., and N. Bauer. 2018. Endothelial extracellular vesicles in pulmonary function and disease. In *Current topics in membranes*. P. Belwiche and S. Dudek, editors. Academic Press, Cambridge, MA. 197–256.
27. Khalyfa, A., L. Kheirandish-Gozal, and D. Gozal. 2018. Exosome and macrophage crosstalk in sleep-disordered breathing-induced metabolic dysfunction. *Int. J. Mol. Sci.* **19**: E3383.
28. Becker, A., B. K. Thakur, J. M. Weiss, H. S. Kim, H. Peinado, and D. Lyden. 2016. Extracellular vesicles in cancer: cell-to-cell mediators of metastasis. *Cancer Cell.* **30**: 836–848.
29. Dieker, J., J. Tel, E. Pieterse, A. Thielen, N. Rother, M. Bakker, J. Fransen, H. B. P. M. Dijkman, J. H. Berden, J. M. de Vries, et al. 2016. Circulating apoptotic microparticles in systemic lupus erythematosus patients drive the activation of dendritic cell subsets and prime neutrophils for NETosis. *Arthritis Rheumatol.* **68**: 462–472.
30. Leal, A. C., D. M. Mizurini, T. Gomes, N. C. Rochael, E. M. Saraiva, M. S. Dias, C. C. Werneck, M. S. Sielski, C. P. Vicente, and R. Q. Monteiro. 2017. Tumor-derived exosomes induce the formation of neutrophil extracellular traps: implications for the establishment of cancer-associated thrombosis. *Sci. Rep.* **7**: 6438.
31. Brinkmann, V., and A. Zychlinsky. 2007. Beneficial suicide: why neutrophils die to make NETs. *Nat. Rev. Microbiol.* **5**: 577–582.
32. Kessenbrock, K., M. Krumbholz, U. Scho, W. Back, W. L. Gross, Z. Werb, V. Brinkmann, D. E. Jenne, U. Schönemarker, and H.J. Gröne. 2009. Netting neutrophils in autoimmune small-vessel vasculitis. *Nat. Med.* **15**: 623–625.
33. Kolaczowska, E., C. N. Jenne, B. G. J. Surewaard, A. Thanabalasuriar, W-Y. Lee, M-J. Sanz, K. Mowen, G. Opdenakker, and P. Kubes. 2015. Molecular mechanisms of NET formation and degradation revealed by intravital imaging in the liver vasculature. *Nat. Commun.* **6**: 6673.
34. Yousefi, S., C. Mihalache, E. Kozłowski, I. Schmid, and H. U. Simon. 2009. Viable neutrophils release mitochondrial DNA to form neutrophil extracellular traps. *Cell Death Differ.* **16**: 1438–1444.
35. Amini, P., D. Stojkov, A. Felser, C. B. Jackson, C. Courage, A. Schaller, L. Gelman, M. E. Soriano, J-M. Nuoffer, L. Scorrano, et al. 2018. Neutrophil extracellular trap formation requires OPA1-dependent glycolytic ATP production. *Nat. Commun.* **9**: 2958.
36. Mulder, A. H., C. A. Stegeman, and C. G. Kallenberg. 1995. Activation of granulocytes by anti-neutrophil cytoplasmic antibodies (ANCA) in Wegener’s granulomatosis: a predominant role for the IgG3 subclass of ANCA. *Clin. Exp. Immunol.* **101**: 227–232.
37. Szczeklik, W., B. Jakiela, K. Wawrzycka-Adamczyk, M. Sanak, M. Hubalewska-Mazgaj, A. Padjas, M. Surmiak, K. Szczeklik, J. Sznajd, and J. Musiał. 2017. Skewing toward Treg and Th2 responses is a characteristic feature of sustained remission in ANCA-positive granulomatosis with polyangiitis. *Eur. J. Immunol.* **47**: 724–733.
38. Kronbichler, A., J. Kerschbaum, G. Gründlinger, J. Leierer, G. Mayer, and M. Rudnicki. 2016. Evaluation and validation of biomarkers in granulomatosis with polyangiitis and microscopic polyangiitis. *Nephrol. Dial. Transplant.* **31**: 930–936.
39. Surmiak, M. P., M. Hubalewska-Mazgaj, K. Wawrzycka-Adamczyk, W. Szczeklik, J. Musiał, and M. Sanak. 2015. Circulating mitochondrial DNA in serum of patients with granulomatosis with polyangiitis. *Clin. Exp. Immunol.* **181**: 150–155.
40. Omann, G. M., A. E. Traynor, A. L. Harris, and L. A. Sklar. 1987. LTB4 induced activation signals and responses in neutrophils are short-lived compared to formylpeptide. *J. Immunol.* **138**: 2626–2632.
41. Gay, J. C., J. K. Beckman, A. R. Brash, J. A. Oates, and J. N. Lukens. 1984. Enhancement of chemotactic factor-stimulated neutrophil oxidative metabolism by leukotriene B4. *Blood.* **64**: 780–785.
42. Norgauer, J., M. Barbisch, W. Czech, J. Pareigis, U. Schwenk, and J. M. Schröder. 1996. Chemotactic 5-oxo-icosatetraenoic acids activate a unique pattern of neutrophil responses. Analysis of phospholipid metabolism, intracellular Ca²⁺ transients, actin reorganization, superoxide-anion production and receptor up-regulation. *Eur. J. Biochem.* **236**: 1003–1009.
43. Powell, W. S., S. Gravel, R. J. MacLeod, E. Mills, and M. Hashefi. 1993. Stimulation of human neutrophils by 5-oxo-6,8,11,14-eicosatetraenoic acid by a mechanism independent of the leukotriene B4 receptor. *J. Biol. Chem.* **268**: 9280–9286.
44. O’Flaherty, J. T., M. Kuroki, A. B. Nixon, J. Wijkander, E. Yee, S. L. Lee, P. K. Smitherman, R. L. Wykle, and L. W. Daniel. 1996. 5-Oxo-eicosanoids and hematopoietic cytokines cooperate in stimulating neutrophil function and the mitogen-activated protein kinase pathway. *J. Biol. Chem.* **271**: 17821–17828.
45. Rhys, H. I., F. Dell’Accio, C. Pitzalis, A. Moore, L. V. Norling, and M. Perretti. 2018. Neutrophil microvesicles from healthy control and rheumatoid arthritis patients prevent the inflammatory activation of macrophages. *EBioMedicine.* **29**: 60–69.
46. Headland, S. E., H. R. Jones, L. V. Norling, A. Kim, P. R. Souza, E. Corsiero, C. D. Gil, A. Nerviani, F. Dell’Accio, C. Pitzalis, et al. 2015. Neutrophil-derived microvesicles enter cartilage and protect the joint in inflammatory arthritis. *Sci. Transl. Med.* **7**: 315ra190.
47. Duche, A-C., L. H. Boudreau, G. S. Naika, J. Bollinger, C. Belleannée, N. Cloutier, B. Laffont, R. E. Mendoza-Villarroel, T. Lévesque, E. Rollet-Labelle, et al. 2015. Platelet microparticles are internalized in neutrophils via the concerted activity of 12-lipoxygenase and secreted phospholipase A2-IIA. *Proc. Natl. Acad. Sci. USA.* **112**: E3564–E3573. [Erratum. 2015. *Proc. Natl. Acad. Sci. USA.* **112**: E6825.]
48. Maugeri, N., P. Rovere-Querini, M. Baldini, E. Baldissera, M. G. Sabbadini, M. E. Bianchi, and A. A. Manfredi. 2014. Oxidative stress elicits platelet/leukocyte inflammatory interactions via HMGB1: a candidate for microvessel injury in systemic sclerosis. *Antioxid. Redox Signal.* **20**: 1060–1074.
49. Maugeri, N., L. Campana, M. Gavina, C. Covino, M. De Matrio, C. Panciroli, L. Maiuri, A. Maseri, A. D’Angelo, M. E. Bianchi, et al. 2014. Activated platelets present high mobility group box

- l to neutrophils, inducing autophagy and promoting the extrusion of neutrophil extracellular traps. *J. Thromb. Haemost.* **12**: 2074–2088.
50. Johnson III, B. L., J. W. Kuethe, and C. C. Caldwell. 2014. Neutrophil derived microvesicles: emerging role of a key mediator to the immune response. *Endocr. Metab. Immune Disord. Drug Targets.* **14**: 210–217.
 51. Boilard, E. 2018. Extracellular vesicles and their content in bioactive lipid mediators: more than a sack of microRNA. *J. Lipid Res.* **59**: 2037–2046.
 52. Sagini, K., E. Costanzi, C. Emiliani, S. Buratta, and L. Urbanelli. 2018. Extracellular vesicles as conveyors of membrane-derived bioactive lipids in immune system. *Int. J. Mol. Sci.* **19**: E1227.
 53. Rådmark, O., and B. Samuelsson. 2009. 5-Lipoxygenase: mechanisms of regulation. *J. Lipid Res.* **50 (Suppl.)**: S40–S45.
 54. Steinhilber, D. 1994. 5-Lipoxygenase: enzyme expression and regulation of activity. *Pharm. Acta Helv.* **69**: 3–14.
 55. Hedi, H., and G. Norbert. 2004. 5-Lipoxygenase pathway, dendritic cells, and adaptive immunity. *J. Biomed. Biotechnol.* **2004**: 99–105.
 56. Majumdar, R., A. Tavakoli Tameh, and C. A. Parent. 2016. Exosomes mediate LTB4 release during neutrophil chemotaxis. *PLoS Biol.* **14**: e1002336.
 57. Powell, W. S., F. Gravelle, and S. Gravel. 1994. Phorbol myristate acetate stimulates the formation of 5-oxo-6,8,11,14-eicosatetraenoic acid by human neutrophils by activating NADPH oxidase. *J. Biol. Chem.* **269**: 25373–25380.
 58. Kowal, K., A. Gielicz, and M. Sanak. 2017. The effect of allergen-induced bronchoconstriction on concentration of 5-oxo-ETE in exhaled breath condensate of house dust mite-allergic patients. *Clin. Exp. Allergy.* **47**: 1253–1262.